Identification of pathways and key genes in male late-stage carotid atherosclerosis using bioinformatics analysis

DI ZHANG[1], XIN LI[1], BEI JING[1], HUIMEI SHI[1], SHIQUAN CHANG[1], ZHENNI CHEN[1], YACHUN ZHENG[1], YUWEI PAN[2], GUOQIANG QIAN[3] and GUOPING ZHAO[1]

[1]College of Traditional Chinese Medicine, Jinan University, Guangzhou, Guangdong 510632; [2]Department of Preventive Treatment of Disease, Tianhe Traditional Chinese Medicine Hospital, Guangzhou, Guangdong 510665; [3]College of Traditional Chinese Medicine, Guangdong Pharmaceutical University, Guangzhou, Guangdong 510006, P.R. China

Abstract. Late-stage carotid atherosclerosis has a high incidence rate and may lead to various cerebrovascular diseases. The gene expression profile GSE100927 was selected to identify differentially expressed genes (DEGs) in carotid atherosclerosis. Subsequently, protein-protein interaction, Gene Ontology and Kyoto Encyclopedia of Genes and Genomes analyses were conducted. Furthermore, experimental verification was performed using human umbilical vein endothelial cells (HUVECs), human aortic vascular smooth muscle cells (HAVSMCs) and Tohoku Hospital Pediatrics-1 (THP-1)-induced macrophages. The groups were as follows: Control group, solvent control group and palmitic acid group. The levels of reactive oxygen species (ROS) in the three cell types were detected by flow cytometry or fluorescence microscopy. Furthermore, apoptosis of HUVECs and HAVSMCs was assessed by flow cytometry and the nuclear Hoechst 33258 staining of THP-1-induced macrophages was performed. Male late-stage carotid atherosclerosis samples, including 10 control samples and 21 atherosclerosis samples, were selected. Pathway enrichment analysis demonstrated that 'Toll-like receptor signaling pathway' was the top pathway associated with the DEGs. MMP7, MMP9, IL1β, C-C motif chemokine ligand 4 (CCL4), secreted phosphoprotein 1 (SPP1), CCL3 and interferon regulatory factor 5 (IRF5) were selected for experimental verification. Palmitic acid increased the ROS levels and the apoptosis rates of HUVECs and HAVSMCs. However, it did not increase the levels of ROS and did not shrink the nuclei of THP-1-induced macrophages. Furthermore, palmitic acid increased the mRNA levels of IL1β, CCL4, SPP1, CCL3, IRF5, MMP7 and MMP9 in HUVECs and THP-1-induced macrophages, and increased the mRNA levels of CCL4 and MMP9 in HAVSMCs. In conclusion, IL1β, CCL3, CCL4, SPP1, IRF5, MMP7 and MMP9 are important markers of late-stage carotid atherosclerosis.

Introduction

Atherosclerosis is a progressive chronic inflammatory and metabolic disease with lipid deposition, focal intimal thickening, smooth muscle cell proliferation and plaque formation (1). With the changes in diet, atherosclerosis and its complications have increased and caused elevated morbidity and mortality worldwide (2). Atherosclerosis of the internal carotid artery, leading to narrowing of the vessel lumen by >50% of the original size, affects nearly 10% of the population above the age of 70 years and causes ~15% of ischemic strokes (3). According to the statistics of patients with carotid atherosclerosis, males are more prone to carotid atherosclerosis and the incidence rate of carotid atherosclerosis in males is higher than that in females (4). Elucidating the mechanisms of male carotid atherosclerosis may help to explain the high incidence rate in males and this may prevent male carotid atherosclerosis in the future.

The mechanisms of atherosclerosis have remained to be fully elucidated. However, lipid metabolism disorders, endothelial dysfunction (5), inflammation (6) and oxidative stress are involved in the formation of atherosclerosis. In the Gene Expression Omnibus (GEO) dataset GSE100927, atherosclerosis was assessed in numerous parts of the human artery,

Correspondence to: Professor Guoping Zhao, College of Traditional Chinese Medicine, Jinan University, 601 Huangpu Avenue West, Guangzhou, Guangdong 510632, P.R. China
E-mail: tguo428@jnu.edu.cn

Dr Guoqiang Qian, College of Traditional Chinese Medicine, Guangdong Pharmaceutical University, 280 Waihuan East Road, Guangzhou, Guangdong 510006, P.R. China
E-mail: gqqian1@163.com

including the atherosclerotic femoral artery, infra-popliteal artery and carotid artery (7). The GSE100927 dataset contains 96 samples, including 31 healthy arterial samples and 65 late-stage atherosclerotic arterial samples. For the present study, the gene expression profile of GSE100927 was selected and the data of 10 male normal samples and 21 male late-stage atherosclerosis samples were acquired. To date, the diagnosis rate of atherosclerotic femoral artery and infra-popliteal artery is less than that of carotid artery. So, carotid atherosclerosis rather than atherosclerotic femoral artery and infra-popliteal artery was selected in this study.

In the present study, key genes in carotid atherosclerosis were screened out via bioinformatics, including MMP7, MMP9, IL1β, C-C motif chemokine ligand 4 (CCL4), secreted phosphoprotein 1 (SPP1), CCL3 and interferon regulatory factor 5 (IRF5). Subsequently, the mRNA levels of these genes were measured in human umbilical vein endothelial cells (HUVECs), human aortic vascular smooth muscle cells (HAVSMCs) and Tohoku Hospital Pediatrics-1 (THP-1)-induced macrophages.

Materials and methods

Data sources. The GSE100927 gene expression dataset was obtained from the GEO database (https://www.ncbi.nlm.nih.gov/gds/), which may be used for genome-wide expression analyses. The gene expression dataset is based on the GPL17077 platform (Agilent-039494 SurePrint G3 Human GE v2 8x60K Microarray 039381). The GSE100927 dataset contains 31 healthy artery samples and 65 atherosclerotic artery samples. Male carotid atherosclerosis samples were selected for analysis, including 10 healthy samples (control samples) and 21 late-stage atherosclerosis samples. The raw data were downloaded as MINiML files. The extracted data were normalized. A fold change of at least 2 and P≤0.05 was considered to indicate a statistically significant difference. A total of 32 upregulated and 13 downregulated genes were identified.

Functional annotation of DEGs using Gene Ontology (GO) and Kyoto Encyclopedia of Genes and Genomes (KEGG) analysis. The cluster Profiler package in R is a tool to implement methods when analyzing and visualizing the functional profiles of genomic coordinates and was used to perform GO and KEGG analysis (8). GO analysis is a useful method, which includes three biological aspects: Biological Process (BP), Molecular Function (MF) and Cellular Component (CC) (9). KEGG is a commonly used bioinformatics database, which analyzes gene functions and enriched genes with their pathways (10,11). The GO and KEGG enrichment analyses were performed for DEGs using the cluster Profiler package. The top 10 terms were selected.

Construction of the protein-protein interaction (PPI) network and Venn diagram. The Search Tool for the Retrieval of Interacting Genes and proteins (STRING) database (https://string-db.org/) may be used for the prediction of PPIs. A total of 45 genes were inputted into STRING. In addition, disconnected nodes in the network were hidden and the minimum required interaction score was 0.700. The line thickness indicated the strength of data support. Genes ranking first

in BP, MF and CC were inputted into a Venn diagram and the common genes were acquired.

Cell lines. Cells were cultured in 5% CO_2 at 36.5±0.5˚C and under 95% relative humidity. HAVSMCs were purchased from Shenzhen Kuyuan Biotechnology Co., Ltd. HUVECs (CL-0122) and THP-1 (CL-0233) cells were purchased from Procell Life Science & Technology Co., Ltd. THP-1 cells were cultured in RPMI-1640 (Gibco; Thermo Fisher Scientific, Inc.) +10% FBS + 0.05 mM β-mercaptoethanol (PB180633) + 1% antibiotics. HAVSMCs and HUVECs were cultured in 10% FBS + 89% DMEM (Gibco; Thermo Fisher Scientific, Inc.) + 1% antibiotics. HAVSMCs, HUVECs and THP-1 cells were immortalized cell lines.

Reagents. RNAiso Plus was acquired from Takara Biotechnology Co., Ltd. SYBR®-Green Premix qPCR, an Evo M-MLV RT-PCR kit and RNase-free water (cat. nos. AG11701, AG11602 and AG11012, respectively) were obtained from Accurate Biotechnology Co., Ltd. 2',7'-dichloro-dihydrofluorescein diacetate (DCFH-DA; cat. no. D6883) and a Cell Counting Kit-8 (CCK-8; cat. no. 96992) were acquired from MilliporeSigma. Hoechst 33342 (cat. no. M5112) was obtained from Guangzhou Juyan Biological Co., Ltd. Palmitic acid and solvent (SYSJ-KJ0040) were acquired from Xi'an Quantum Technology Development Co., Ltd. The Annexin V APC Apoptosis Detection Kit I (cat. no. 62700-80) was purchased from Guangzhou Squirrel Biological Co., Ltd.

Cell viability and cytotoxicity assays. The viability of cells was determined using a CCK-8 assay. First, all cells were seeded into 96-well plates at a density of $6x10^3$ cells/well and incubated for 24 h. To assess the effect of palmitic acid, the cells were then incubated with palmitic acid at various concentrations (0, 25, 50, 75, 100, 125, 150, 175 or 200 μM) for 6, 12, 24 or 36 h, and then subjected to the CCK-8 assay at 37˚C for 1 h. The absorbance at 450 nm was measured using a microplate reader (BioTek Instruments, Inc.).

Experimental grouping. The groups were as follows: Control group, solvent control group (equal volume of solvent) and palmitic acid group (200 μM palmitic acid). Following co-cultivation with palmitic acid for 24 h, cells were used in a series of experiments.

Intracellular reactive oxygen species (ROS) measurement. Cells ($1x10^6$) in a 6-well plate or collected in an Eppendorf tube were incubated at 37˚C for 20 min in PBS containing 20 μM DCFH-DA. After the DCFH-DA was removed, cells were washed three times with PBS. Subsequently, intracellular ROS production was measured using an inverted fluorescence microscope (Axio Vert.A1; Carl Zeiss, Inc.) or a flow cytometer (CytExpert 2.3; Beckman Coulter, Inc.).

Cell apoptosis detection via flow cytometry. Annexin V allophycocyanin (APC) and PI were used to evaluate the apoptotic rates of cells in different groups. Cells were collected with trypsin (Gibco; Thermo Fisher Scientific, Inc.) and washed with PBS. Subsequently, $1x10^6$ cells were placed in binding buffer and double-stained with Annexin V-allophycocyanin and propidium

Table I. Primer sequences used for PCR.

Gene	Forward primer (5'-3')	Reverse primer (5'-3')
IL1β	ATGATGGCTTATTACAGTGGCAA	GTCGGAGATTCGTAGCTGGA
CCL3	AGTTCTCTGCATCACTTGCTG	CGGCTTCGCTTGGTTAGGAA
CCL4	TCGCAACTTTGTGGTAGA	TTCAGTTCCAGGTCATACAC
IRF5	GGGCTTCAATGGGTCAACG	GCCTTCGGTGTATTTCCCTG
MMP7	GAGTGAGCTACAGTGGGAACA	CTATGACGCGGGAGTTTAACAT
MMP9	GGGACGCAGACATCGTCATC	TCGTCATCGTCGAAATGGGC
SPP1	GAAGTTTCGCAGACCTGACAT	GTATGCACCATTCAACTCCTCG
β-actin	GGGAAATCGTGCGTGACATTAAGG	CAGGAAGGAAGGCTGGAAGAGTG

CCL3, C-C motif chemokine ligand 3; IRF5, interferon regulatory factor 5; SPP1, secreted phosphoprotein 1.
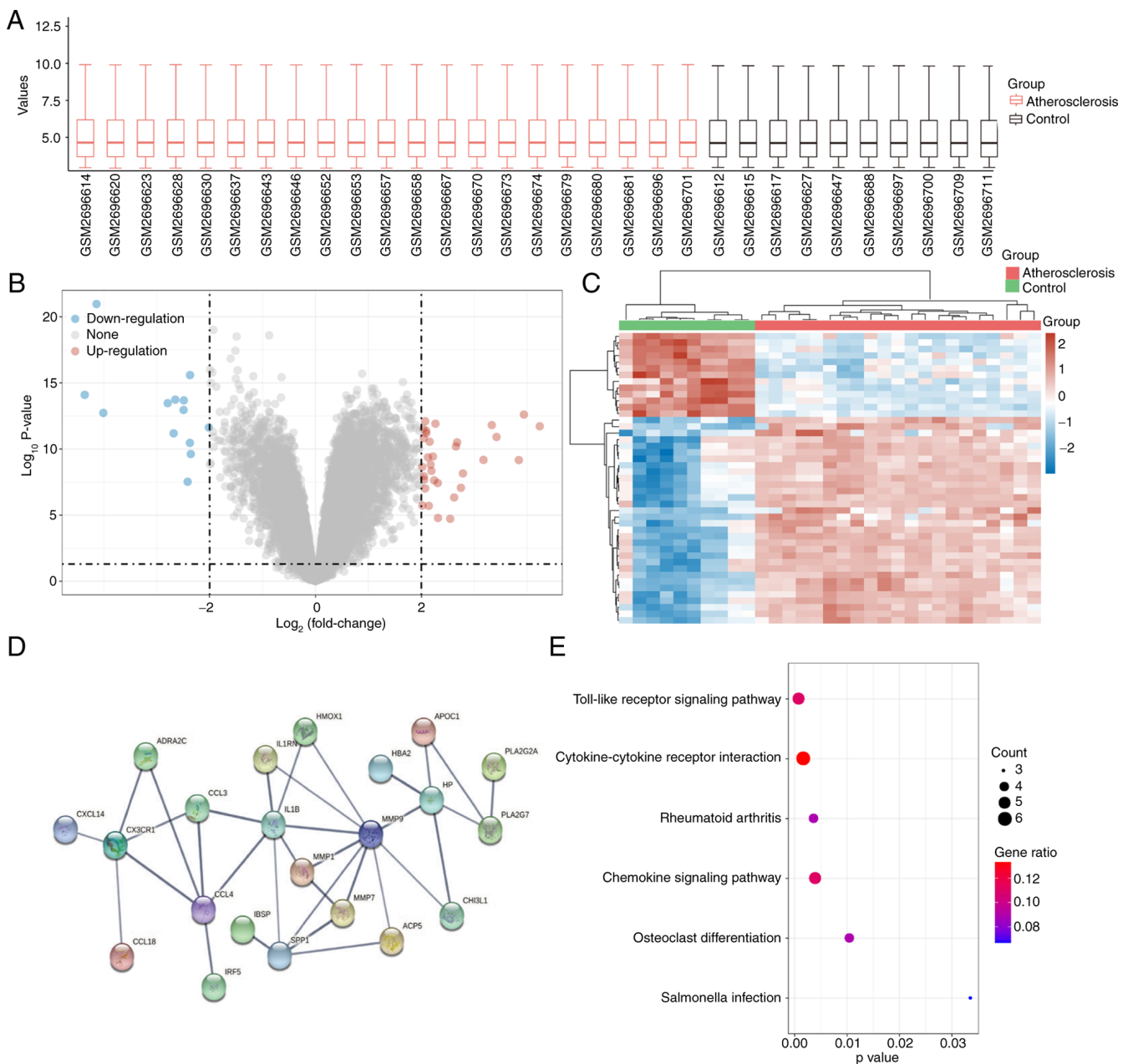

Figure 1. DEGs in carotid atherosclerosis. (A) Expression levels of each sample from the perspective of the overall dispersion of expression. (B) Volcano plot of DEGs (P≤0.05 and |log2|≥2). (C) Clustered heat map. (D) Interrelations between proteins. (E) Enrichment of signaling pathways. DEG, differentially expressed gene.
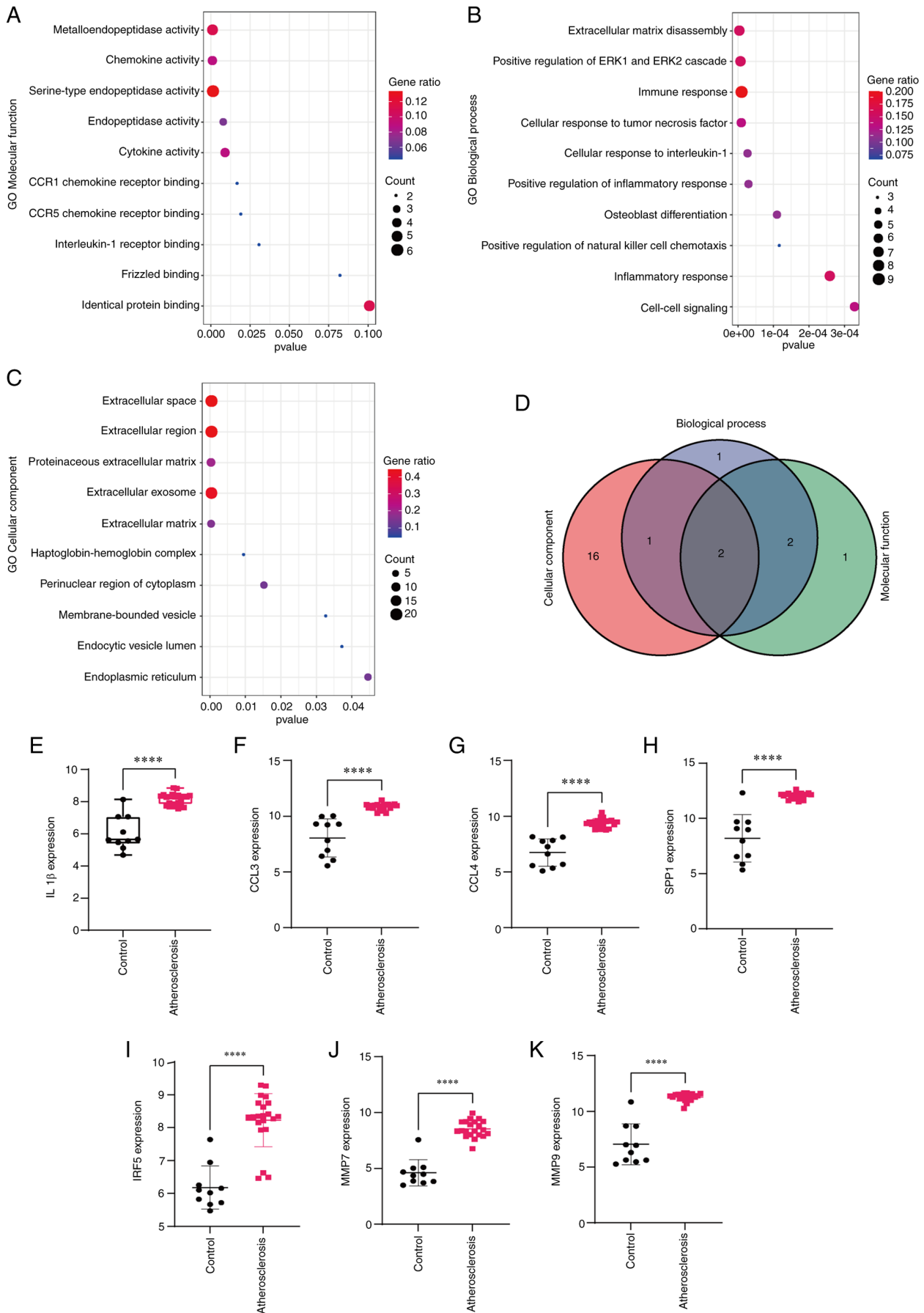
Figure 2. Functional enrichment analysis of differentially expressed genes. GO annotation, including (A) Molecular Function, (B) Biological Process and (C) Cellular Component. (D) Venn diagram for two genes (MMP7 and MMP9) involved in three vital GO annotations. (E-K) Expression levels of (E) IL1β, (F) CCL3, (G) CCL4, (H) SPP1, (I) IRF5, (J) MMP7 and (K) MMP9 in the control and atherosclerosis groups. ****$P < 0.05$. CCL3, C-C motif chemokine ligand 3; CCR1, C-C motif chemokine receptor 1; GO, Gene Ontology; IRF5, interferon regulatory factor 5; SPP1, secreted phosphoprotein 1.

Table II. Kyoto Encyclopedia of Genes and Genomes pathway enrichment.

Term	Pathway	P-value	Genes
hsa04620	Toll-like receptor signaling pathway	0.0004	IL1B, CCL4, SPP1, CCL3, IRF5
hsa04060	Cytokine-cytokine receptor interaction	0.0013	CX3CR1, IL1B, CCL4, CCL3, CCL18, CXCL14
hsa05323	Rheumatoid arthritis	0.0034	MMP1, IL1B, CCL3, ACP5
hsa04062	Chemokine signaling pathway	0.0036	CX3CR1, CCL4, CCL3, CCL18, CXCL14
hsa04380	Osteoclast differentiation	0.0102	FCGR3A, IL1B, ACP5, TREM2
hsa05132	Salmonella infection	0.0334	IL1B, CCL4, CCL3

Table III. GO annotation (biological process, top 10).

Term	Pathway	P-value	Genes
GO:0022617	Extracellular matrix disassembly	3.24073×10^{-8}	MMP12, MMP7, MMP1, SPP1, ADAM8, CAPG, MMP9
GO:0070374	Positive regulation of ERK1 and ERK2 cascade	4.51858×10^{-6}	HAND2, PLA2G2A, CCL4, CCL3, CHI3L1, TREM2, CCL18
GO:0071356	Cellular response to tumor necrosis factor	7.71998×10^{-6}	SFRP1, CCL4, CCL3, CHI3L1, CCL18, HAMP
GO:0006955	Immune response	8.16275×10^{-6}	IL1RN, FCGR3A, IL1B, AQP9, CCL4, CCL3, CCL18, HAMP, CXCL14
GO:0071347	Cellular response to interleukin-1	2.90881×10^{-5}	SFRP1, CCL4, CCL3, CHI3L1, CCL18
GO:2000503	Positive regulation of natural killer cell chemotaxis	1.2724×10^{-4}	CCL4, CCL3, CXCL14
GO:0001649	Osteoblast differentiation	1.29681×10^{-4}	SFRP1, IBSP, MYOC, SPP1, CCL3
GO:0006954	Inflammatory response	3.3532×10^{-4}	IL1B, CCL4, SPP1, CCL3, CHI3L1, ADAM8, CCL18
GO:0007267	Cell-cell signaling	4.09983×10^{-4}	IL1B, CCL4, CCL3, ADRA2C, CCL18, CXCL14
GO:0045780	Positive regulation of bone resorption	4.68124×10^{-4}	CA2, SPP1, ADAM8

GO, Gene Ontology.

iodide in the dark for 15 min at 4˚C. The proportion of apoptotic cells was then analyzed on a flow cytometer (CytExpert 2.3; Beckman Coulter, Inc.) to determine the apoptotic rate.

Hoechst 33258 staining. Cells were incubated for 20 min with 5 μl Hoechst 33258 in 0.995 ml PBS at 37˚C. After washing twice with PBS, the fluorescence images were captured using an inverted fluorescence microscope (Axio Vert.A1; Carl Zeiss, Inc.), and Image-Pro Plus 6.0 (Media Cybernetics, Inc.) was used for analysis to measure the fluorescence intensity.

Reverse transcription-quantitative PCR (RT-qPCR). According to the manufacturer's protocol, total RNA from cells was isolated using RNAiso Plus. Subsequently, cDNA was synthesized based on the instructions of the RT-PCR kit (catalog no. AG11602). Subsequently, a Bio-Rad CFX96 Real-Time PCR System (Bio-Rad Laboratories, Inc.) was used to perform qPCR. The amplification parameters were as follows: 95˚C for 30 sec, followed by 40 cycles of 95˚C for 5 sec and 60˚C for 34 sec, 95˚C for 15 sec, 60˚C for 60 sec and 95˚C for 15 sec. Relative mRNA expression was calculated using the $2^{-\Delta\Delta Cq}$ method after normalization to β-actin (12,13). For this procedure, SYBR®-Green Premix qPCR and primers (Table I) were used.

Statistical analysis. Values are expressed as the mean ± standard deviation. The experiments were repeated three times. GraphPad Prism 8 (GraphPad Software, Inc.) was used to perform statistical analysis. The data were analyzed by one-way ANOVA. Bonferroni's test was used as the post-hoc test after ANOVA. P<0.05 was considered to indicate a statistically significant difference.

Results

Genes detected in DEG analysis and interaction diagram of proteins. DEG analysis was performed on the GSE100927 dataset (Fig. 1A). The extracted data were processed by log2 transformation, and P≤0.05 was deemed significant. A total of 32 upregulated and 13 downregulated genes were identified (Fig. 1B). The expression matrices of the identified genes were selected from the GSE100927 dataset and the clustered heat

Table IV. GO annotation (cellular component, top 10).

Term	Pathway	P-value	Genes
GO:0005615	Extracellular space	1.0927×10^{-11}	IL1RN, SPON1, MMP7, MYOC, PLA2G2A, HP, CXCL14, MMP9, SFRP1, IBSP, CA2, IL1B, CCL4, SPP1, CCL3, HMOX1, CHI3L1, APOD, CCL18, SCRG1, HAMP
GO:0005576	Extracellular region	1.64812×10^{-8}	MMP7, MMP1, PLA2G2A, HP, HBA2, TREM2, CXCL14, MMP9, MMP12, IL4I1, SFRP1, IBSP, IL1B, CCL4, APOC1, SPP1, CCL3, APOD, HAMP
GO:0005578	Proteinaceous extracellular matrix	2.65218×10^{-7}	MMP12, SPON1, SFRP1, MMP7, MYOC, MMP1, TFPI2, CHI3L1, MMP9
GO:0070062	Extracellular exosome	1.48988×10^{-5}	IL1RN, MMP7, MYOC, PLA2G2A, HP, HBA2, CAPG, MMP9, FCGR3A, SFRP1, DES, CA2, IL1B, APOC1, SPP1, ACP5, CHI3L1, APOD, PI16, FBP1
GO:0031012	Extracellular matrix	8.34484×10^{-5}	SPON1, SFRP1, MMP7, IBSP, MYOC, MMP1, TFPI2
GO:0031838	Haptoglobin-hemoglobin complex	9.841369×10^{-3}	HP, HBA2
GO:0048471	Perinuclear region of cytoplasm	1.7958995×10^{-2}	CX3CR1, PLA2G2A, SPP1, HMOX1, CHI3L1, APOD
GO:0031988	Membrane-bounded vesicle	3.4032333×10^{-2}	IBSP, SPP1
GO:0071682	Endocytic vesicle lumen	3.8800705×10^{-2}	HP, HBA2
GO:0005783	Endoplasmic reticulum	5.2251773×10^{-2}	MYOC, APOC1, PLA2G2A, HMOX1, CHI3L1, APOD

GO, Gene Ontology.

Table V. GO annotation (molecular function, top 10).

Term	Pathway	P-value	Genes
GO:0004222	Metalloendopeptidase activity	0.000159247	MMP12, MMP7, MMP1, ADAM8, MMP9
GO:0008009	Chemokine activity	0.000226706	CCL4, CCL3, CCL18, CXCL14
GO:0004252	Serine-type endopeptidase activity	0.000363433	MMP12, MMP7, MMP1, HP, ADAM8, MMP9
GO:0004175	Endopeptidase activity	0.007603833	MMP12, MMP1, MMP9
GO:0005125	Cytokine activity	0.008882175	IL1RN, IL1B, CCL4, SPP1
GO:0031726	CCR1 chemokine receptor binding	0.016880964	CCL4, CCL3
GO:0031730	CCR5 chemokine receptor binding	0.019269721	CCL4, CCL3
GO:0005149	Interleukin-1 receptor binding	0.031128822	IL1RN, IL1B
GO:0042802	Identical protein binding	0.033983341	SFRP1, DES, CCL4, CCL3, FBP1, MMP9
GO:0005109	Frizzled binding	0.083902905	SFRP1, MYOC

GO, Gene Ontology; CCR1, C-C motif chemokine receptor 1.

map was constructed using the heatmap function (Fig. 1C). A total of 45 genes were inputted into STRING and the PPI relationship was determined (Fig. 1D).

Functional enrichment analysis of DEGs. The top 10 significant terms in the GO annotation (Fig. 2A-C) and 6 most significant terms in the pathway enrichment analysis (Fig. 1E; Table II) were identified. The results of the pathway enrichment analysis revealed that the 'Toll-like receptor signaling pathway' ranked first and this was selected for experimental verification (Fig. 1E). As for the GO annotation,

the terms ranking first in BP (Table III), CC (Table IV) and MF (Table V) were selected. The Venn diagram indicated two genes (MMP7 and MMP9) that were involved in these three categories of terms. Subsequently, the expression levels of IL1β, CCL4, SPP1, CCL3, IRF5, MMP7 and MMP9 were examined. The results indicated that IL1β, CCL4, SPP1, CCL3, IRF5, MMP7 and MMP9 were highly expressed in the atherosclerosis group (Fig. 2E-K).

Palmitic acid affects cell viability. To examine the cytotoxicity of palmitic acid, HUVECs, HAVSMCs and THP-1-induced
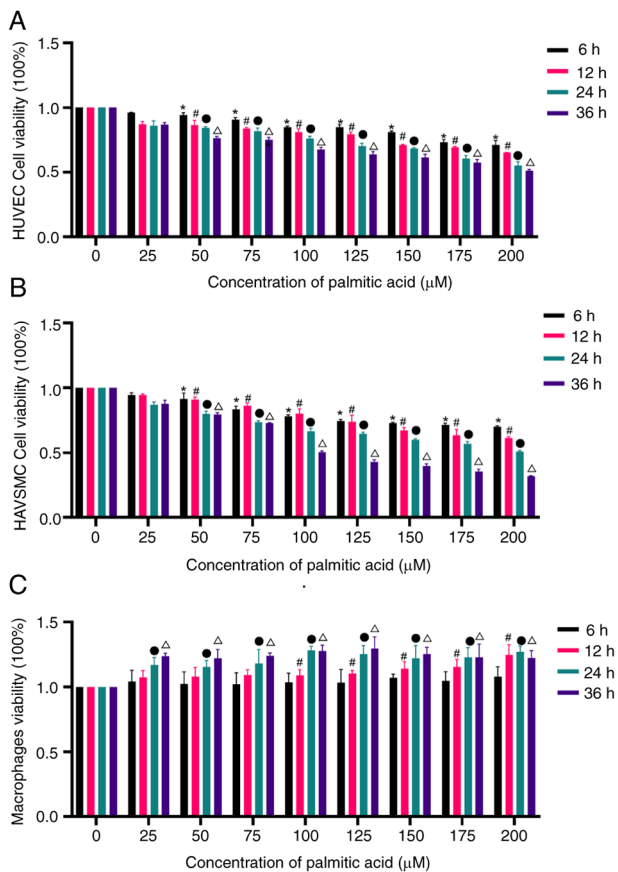
Figure 3. Palmitic acid affects cell viability. Effects of palmitic acid on the viability of (A) HUVECs, (B) HAVSMCs and (C) Tohoku Hospital Pediatrics-1-induced macrophages. *, #, ● and Δ indicate P<0.05 compared with the 0 μM group at 6, 12, 24 and 36 h at the same time-point. HUVEC, human umbilical vein endothelial cell; HAVSMC, human aortic vascular smooth muscle cell.

macrophages were incubated with different doses of palmitic acid in the culture medium containing 10% FBS for 6, 12, 24 or 36 h. Cytotoxicity/growth inhibition was determined by a CCK-8 assay. Palmitic acid (50, 75, 100, 125, 150, 175 or 200 μM) significantly lowered the viability of HUVECs and HAVSMCs at different time-points (P<0.05; Fig. 3A and B), with a maximum response at 200 μM, while 100, 125, 150, 175 and 200 μM palmitic acid increased the viability of THP-1-induced macrophages at different time-points (P<0.05) with a maximum response at 200 μM (Fig. 3C). Since incubation with 200 μM palmitic acid for 36 h markedly decreased cell viability and was associated with increased cell death, incubation with 200 μM palmitic acid for 24 h was considered more suitable.

Palmitic acid induces ROS production of cells. To determine whether palmitic acid has an effect on intracellular oxidative stress, it was investigated whether palmitic acid had effects on the production of ROS in cells. Intracellular ROS levels in the different groups of cells were examined after incubation with palmitic acid for 24 h via fluorescence microscopy and flow cytometry. As indicated in Fig. 4Aa-d, incubation with palmitic acid increased intracellular ROS levels of HUVECs (P<0.05), while the solvent alone did not. As presented in Fig. 4Ba-d, incubation with palmitic acid increased intracellular ROS

levels of HAVSMCs (P<0.05), while the solvent alone had no such effect. Of note, palmitic acid and solvent incubation did not change the ROS levels of THP-1-induced macrophages (Fig. 4Ca-b).

Effects of palmitic acid on cell apoptosis. Certain studies have reported the use of palmitic acid to represent athero-sclerosis (14,15). To determine the damaging effects of palmitic acid, it was investigated whether palmitic acid had effects on cell apoptosis and cell nuclear changes. In the present study, cell apoptosis was examined after incubation with palmitic acid for 24 h via fluorescence microscopy and nuclear changes were observed via Hoechst 33258 staining. As presented in Fig. 5A and B, palmitic acid increased the proportion of apoptotic HAVSMCs (P<0.05), while the solvent alone did not. Palmitic acid also increased the apoptosis rate of HUVECs (P<0.05), while the solvent did not (Fig. 5C and D). However, palmitic acid and solvent did not affect the nuclei of THP-1-induced macrophages (Fig. 5E and F), as the fluorescence intensity did not vary in the three groups.

mRNA levels of IL1β, CCL4, SPP1, CCL3, IRF5, MMP7 and MMP9. The mRNA expression levels of IL1β, CCL4, SPP1, CCL3, IRF5, MMP7 and MMP9 were detected in HAVSMCs, HUVECs and THP-1-induced macrophages (Fig. 6). Palmitic acid increased the levels of IL1β, CCL4, SPP1, CCL3, IRF5, MMP7 and MMP9 both in THP-1-induced macrophages and HUVECs (P<0.05). In addition, palmitic acid increased the levels of CCL4 and MMP9 (P<0.05), while the expression levels of IRF5 were only slightly altered.

Discussion

Atherosclerosis may occur throughout the arterial vascular system and lead to various diseases. The present study provided evidence that inflammation markers serve a vital role in male late-stage carotid atherosclerosis. The major findings were as follows: i) Carotid atherosclerosis is closely related to arterial inflammation, including pathways such as 'Toll-like receptor signaling pathway', 'Cytokine-cytokine receptor interaction' and 'Chemokine signaling pathway'; ii) macrophages and vascular endothelial cells are involved in vascular inflam-mation; iii) palmitic acid causes apoptosis of HUVECs and HAVSMCs, indicating that hyperlipidemia may cause blood vessel damage, while it does not affect THP-induced macro-phages; and iv) palmitic acid increased the levels of oxidative stress in HUVECs and HAVSMCs, while it did not increase the levels of oxidative stress in THP-induced macrophages.

Steenman *et al* (7) performed a canonical pathway analysis, revealing the important involvement of immune system processes in atherosclerotic and healthy carotid arteries. In the original study providing the GSE100927 dataset, it was demonstrated that the immune system served a key role in atherosclerosis. MMP7 was the top differentially expressed gene between the three arterial territories in both atheroscle-rotic and healthy arteries and carotid atherosclerosis displayed higher expression levels of MMP7, MMP9 and MMP12 than those in the atherosclerotic femoral artery and infra-popliteal artery (7). In the present study, MMP7 and MMP9 were indicated to be involved in biological aspects of carotid
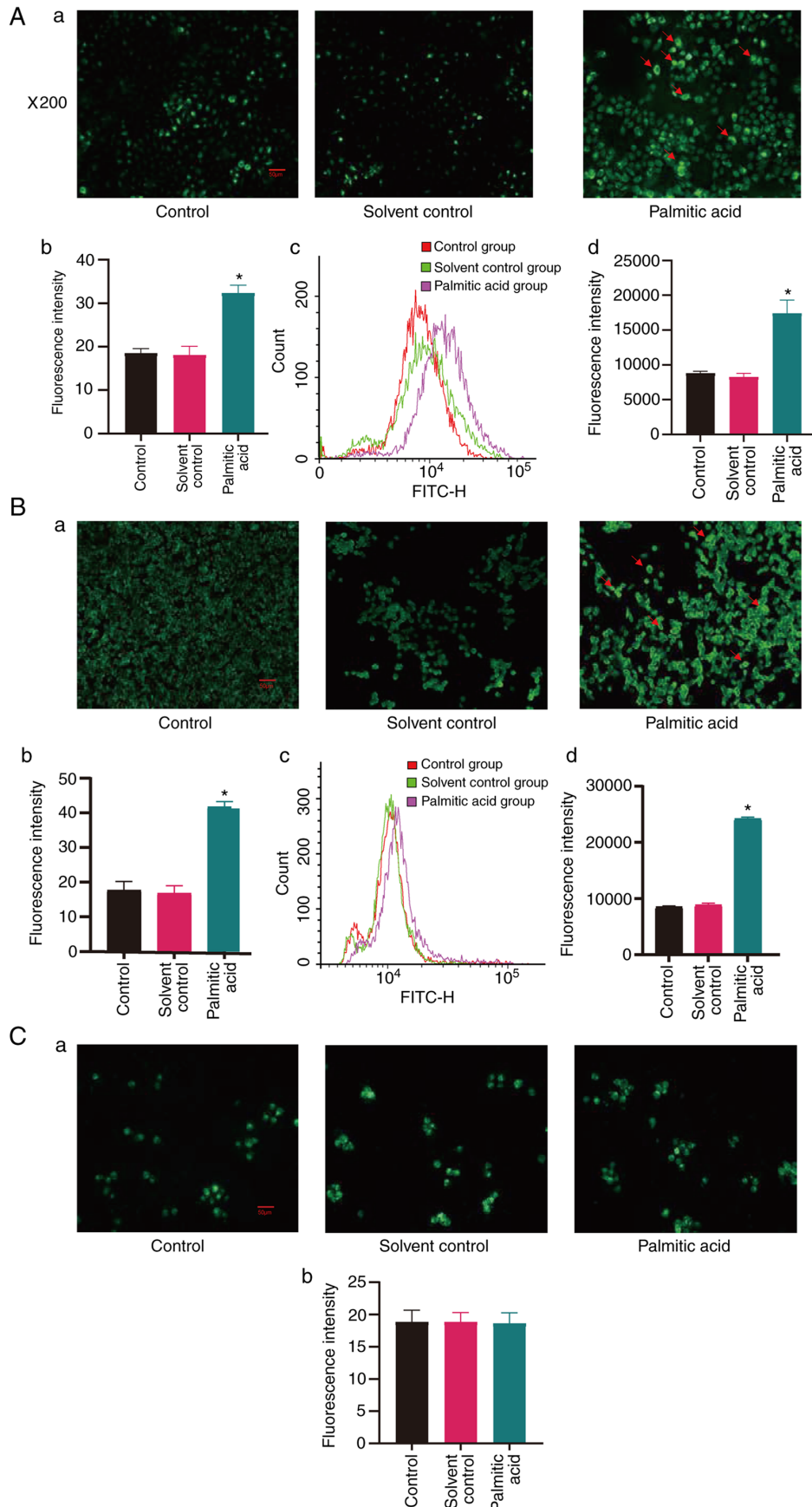
Figure 4. Palmitic acid promotes ROS production in cells. (A) Palmitic acid increased intracellular ROS levels in HUVECs. (Aa) ROS fluorescence (magnification, x200; scale bar, 50 μm) and (Ab) quantified results. (Ac) Flow cytometry histograms and (Ad) results of statistical analysis. (B) Palmitic acid stimulation for 24 h increased ROS levels of human aortic smooth muscle cells. (Ba) ROS fluorescence (magnification, x200; scale bar, 50 μm) and (Bb) quantified results. (Bc) Flow cytometry histograms and (Bd) results of statistical analysis. (C) Palmitic acid and solvent incubation did not affect the ROS levels of Tohoku Hospital Pediatrics-1-induced macrophages. (Ca) Fluorescence (magnification, x200; scale bar, 50 μm) and (Cb) results of statistical analysis. *P<0.05 compared with the control group. ROS, reactive oxygen species.
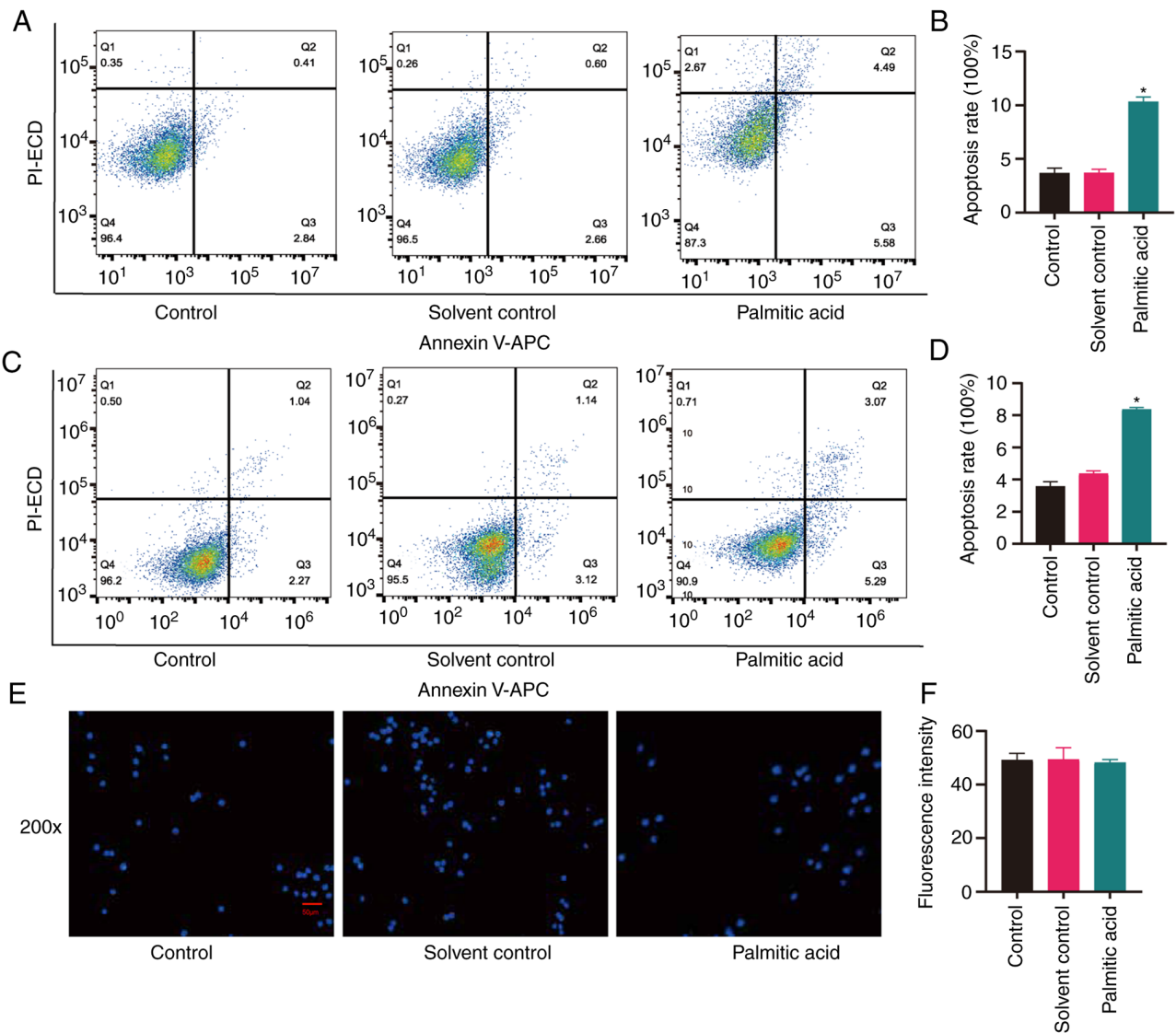
Figure 5. Palmitic acid affects cell apoptosis and has no effect on nuclear changes. (A-D) Incubation with palmitic acid led to apoptosis of HAVSMCs and HUVECs. (A) Flow cytometry dot plot for HAVSMCs and (B) quantified apoptosis rates. (C) Flow cytometry dot plot for HUVECs and (D) quantified apoptosis rates. (E and F) Palmitic acid did not affect the nuclear morphology of Tohoku Hospital Pediatrics-1-induced macrophages. (E) Fluorescence microscopy images for Hoechst 33258 staining and (F) quantified fluorescence intensity (magnification, x200; scale bar, 50 μm). *P<0.05 compared with the control group. APC, allophycocyanin; PI, propidium iodide; Q, quadrant; HUVEC, human umbilical vein endothelial cell; HAVSMC, human aortic vascular smooth muscle cell.

atherosclerosis and were higher expressed after palmitic acid treatment, which was consistent with the results of GSE100927.

The pathogenesis of atherosclerosis is closely related to hyperlipidemia. Free fatty acids may cause endothelial damage and lipid deposition. The effect of palmitic acid on endothelial cells, smooth muscle cells and macrophages is able to induce the high-fat model *in vitro* (14,15). Palmitic acid may lead to inflammation and apoptosis of vascular endothelial cells by mediating the PI3K/Akt/endothelial nitric oxide synthase signaling pathway (16). Palmitic acid induced endothelial lipotoxicity and lectin-like oxidized LDL receptor-1 upregulation by reducing endoplasmic reticulum stress in HUVECs. High glucose- and palmitic acid-induced apoptosis, oxidative stress and inflammatory response in HUVECs (17). Nearly all studies included inflammation, and oxidative stress was involved as well. Thus, inhibiting inflammation requires further investigation in future experiments.

Oxidative stress serves a vital role in the process of atherosclerotic plaque formation (18). Oxidative stress is associated with systemic inflammation, endothelial cell proliferation and apoptosis, as well as vasoconstriction, which contribute to endothelial dysfunction, leading to atherosclerosis (19). Toualbi *et al* (20) suggested that cardiovascular diseases, mainly atherosclerosis, may be diagnosed indirectly by measuring oxidative stress markers. In addition, oxidative stress and inflammation are two major proatherogenic factors, responsible for the modification of vascular wall integrity (21). The present study revealed that palmitic acid may induce increased levels of oxidative stress in HUVECs and HAVSMCs, which is consistent with previous research. Furthermore, attenuating oxidative stress may potentially decelerate the progression of atherosclerotic plaque formation (22). Ji *et al* (23) revealed that propolis ameliorated restenosis in hypercholesterolemia rabbits with carotid
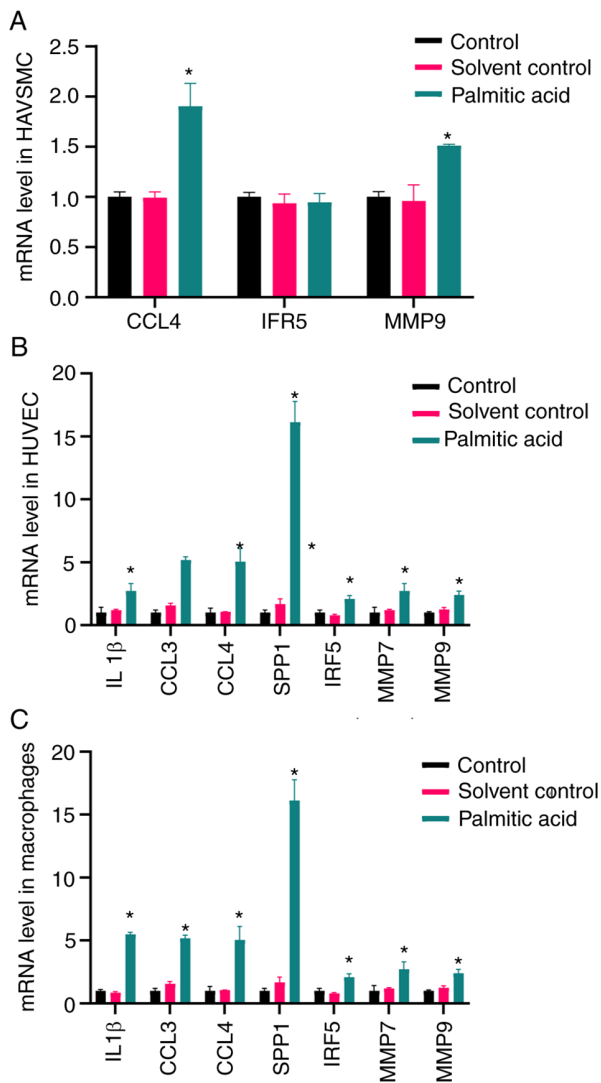
Figure 6. mRNA expression levels of IL1β, CCL4, SPP1, CCL3, IRF5, MMP7 and MMP9. (A) Palmitic acid increased the levels of CCL4 and MMP9, while the levels of IRF5 were not significantly altered. Palmitic acid increased the levels of IL1β, CCL4, SPP1, CCL3, IRF5, MMP7 and MMP9 both in (B) HUVECs and (C) Tohoku Hospital Pediatrics-1-induced macrophages. *P<0.05 compared with the control group. CCL3, C-C motif chemokine ligand 3; HAVSMC, human aortic vascular smooth muscle cell; HUVEC, human umbilical vein endothelial cell; IRF5, interferon regulatory factor 5; SPP1, secreted phosphoprotein 1.

balloon injury by inhibiting lipid accumulation, oxidative stress and the Toll-like receptor 4/NF-κB signaling pathway. Zhang *et al* (24) reported that quercetin is a potential therapeutic agent ameliorating atherosclerotic pathophysiology in rat carotid arteries by inhibiting oxidative stress and inflammatory response, the mechanism of which involved modulating the AMP-activated protein kinase/sirtuin 1/NF-κB signaling pathway. Overproduction of ROS was reported to cause vascular endothelial damage (11,13,25). Endothelial dysfunction-induced lipid retention is an early feature of atherosclerotic lesion formation (26). Apoptosis of vascular smooth muscle cells is one of the major modulating factors of atherogenesis, which accelerates atherosclerosis progression by causing plaque destabilization and rupture (27). The present study revealed that palmitic acid induces apoptosis of HUVECs and HAVSMCs, which

may induce arterial lipid accumulation and exacerbation of atherosclerosis.

Inflammation is one of the major proatherogenic factors, destroying the structure of blood vessels (21). IL1 is a critical factor in the process of atherosclerosis. Mice with knockout of apolipoprotein E (ApoE) and IL1β have markedly smaller sizes of atherosclerotic lesions in the aortic sinus and ratios of atherosclerotic areas of the aorta compared with single ApoE-knockout mice (28). Furthermore, artificial IL1β expression on one side of the coronary artery led to increases in coronary stenosis and aggravation of vascular diseases (29). The present study demonstrated that the expression levels of IL1β in the control group were higher than those in other groups in HUVECs and THP-1 induced macrophages, which was consistent with the previous conclusions.

The circulating levels of C-C chemokine ligand (CCL) are increased in atherosclerotic patients (30). CCL4 may be detected in T-cells, smooth muscle cells and macrophages in atherosclerotic plaques (31), and is further upregulated in vulnerable plaques (32). In the present study, the levels of CCL4 in HAVSMCs, HUVECs and THP-1-induced macrophages were determined. Chang *et al* (31) considered that direct inhibition of CCL4 stabilized atheroma and reduced endothelial and macrophage activation. Komissarov *et al* (33) reported that T-cell migration into human atherosclerotic plaques may predominantly occur via C-C motif chemokine receptor 5-CCL3 and C-X3-C motif chemokine receptor 1-C-X3-C motif chemokine ligand 1 interactions. Munjal and Khandia (34) suggested that the chemokines (family of small cytokines) involved in atherosclerotic plaque formation are CCL3, chemokine (C-X-C motif) ligand 4 and macrophage migration-inhibitory factor. Bai *et al* (35) indicated that the serum levels of SPP1, CD36, ATPase H+ transporting V0 subunit d2, chitinase 3 like 1, myosin heavy chain 11 and brain-derived neurotrophic factor in patients with coronary heart disease differed from those in healthy subjects. The present study revealed that the levels of CCL3 and SPP1 in HUVECs and THP-1-induced macrophages were higher than those in the control group, which was consistent with these reports.

IRF5 serves a central role in inflammation, mediating the production of proinflammatory cytokines, such as IL6, IL12, IL23 and TNF-α (36). Seneviratne *et al* (37) and Posadas-Sanchez *et al* (38) reported that IRF5 was detrimental in atherosclerosis, promoting the maintenance of proinflammatory CD11c+ macrophages. Gaubatz *et al* (39) suggested a positive association between MMP-7 and the calcification of the carotid arteries. Polonskaya *et al* (40) considered that the relative risk of coronary artery calcification was associated with MMP-9 and the MMP-7 levels were markedly higher in patients with coronary heart disease and verified coronary artery atherosclerosis than in the control group. The present results were consistent with these reports.

There are certain deficiencies in the present study. It was not possible to obtain male primary endothelial cells, VSMCs and macrophages to perform validation *in vitro*; thus, HVSMC, HUVEC and THP-1 cell lines were used. These cell lines are more widely used in cardiovascular disease, although these three cell types do not optimally represent the carotid artery. It may be attempted to generate stable male cell cultures in the future. Furthermore, pre-term and mid-term atherosclerosis

was not investigated in the present study. These dynamic processes should be included in future research.

In conclusion, inflammation is closely related to atherosclerosis, as demonstrated using bioinformatics and experimental verification. IL1β, CCL3, CCL4, SPP1, IRF5, MMP7 and MMP9 are markers of carotid atherosclerosis.

Availability of data and materials

The datasets used and/or analyzed during the current study are available from the corresponding author on reasonable request. The gene expression datasets generated and/or analyzed during the current study are available in the GEO repository, https://www.ncbi.nlm.nih.gov/geo/query/acc.cgi?acc=GSE100927.

Authors' contributions

DZ and GZ designed the experiments and wrote this manuscript. GQ was involved in the experimental design and manuscript revision. DZ, BJ and XL completed the experiments. HS, SC, ZC, YZ and YP provided help with the English language revision and were involved in data analysis. DZ, XL, BJ, GQ and GZ confirmed the authenticity of the data. All authors read and approved the final manuscript.

Ethics approval and consent to participate

Not applicable.

Patient consent for publication

Not applicable.

Competing interests

The authors declare that they have no competing interests.

References

1. Kraaijenhof JM, Hovingh GK, Stroes ESG and Kroon J: The iterative lipid impact on inflammation in atherosclerosis. Curr Opin Lipidol 32: 286-292, 2021.
2. Barrett TJ: Macrophages in atherosclerosis regression. Arterioscler Thromb Vasc Biol 40: 20-33, 2020.
3. Arba F, Vit F, Nesi M, Rinaldi C, Silvestrini M and Inzitari D: Carotid revascularization and cognitive impairment: The neglected role of cerebral small vessel disease. Neurol Sci 43: 139-152, 2022.
4. Sinning C, Wild PS, Echevarria FM, Wilde S, Schnabel R, Lubos E, Herkenhoff S, Bickel C, Klimpe S, Gori T, et al: Sex differences in early carotid atherosclerosis (From The Community-Based Gutenberg-Heart Study). Am J Cardiol 107: 1841-1847, 2011.
5. Arnlov J, Sang Y, Ballew SH, Vaidya D, Michos ED, Jacobs DR Jr, Lima J, Shlipak MJ, Bertoni AG, Coresh J, et al: Endothelial dysfunction and the risk of heart failure in a community-based study: The multi-ethnic study of atherosclerosis. ESC Heart Fail 7: 4231-4240, 2020.
6. Ji E and Lee S: Antibody-based therapeutics for atherosclerosis and cardiovascular diseases. Int J Mol Sci 22: 5770, 2021.
7. Steenman M, Espitia O, Maurel B, Guyomarch B, Heymann MF, Pistorius MA, Ory B, Heymann D, Houlgatte R, Gouëffic Y and Quillard T: Identification of genomic differences among peripheral arterial beds in atherosclerotic and healthy arteries. Sci Rep 8: 3940, 2018.
8. Yu G, Wang LG, Han Y and He QY: Clusterprofiler: An R package for comparing biological themes among gene clusters. OMICS 16: 284-287, 2012.
9. Gene Ontology Consortium: The gene ontology (GO) project in 2006. Nucleic Acids Res 34: D322-D326, 2006.
10. Altermann E and Klaenhammer TR: Pathwayvoyager: Pathway mapping using the kyoto encyclopedia of genes and genomes (KEGG) database. BMC Genomics 6: 60, 2005.
11. Zhang D, Yang B, Chang SQ, Ma SS, Sun JX, Yi L, Li X, Shi HM, Jing B, Zheng YC, et al: Protective effect of paeoniflorin on H2O2 induced Schwann cells injury based on network pharmacology and experimental validation. Chin J Nat Med 19: 90-99, 2021.
12. Livak KJ and Schmittgen TD: Analysis of relative gene expression data using real-time quantitative PCR and the 2 (-Delta Delta C(T)) method. Methods 25: 402-408, 2001.
13. Zhang D, Sun J, Chang S, Li X, Shi H, Jing B, Zheng Y, Lin Y, Qian G, Pan Y and Zhao G: Protective effect of 18 beta-glycyrrhetinic acid against H2O2-induced injury in schwann cells based on network pharmacology and experimental validation. Exp Ther Med 22: 1241, 2021.
14. Karbasforush S, Nourazarian A, Darabi M, Rahbarghazi R, Khaki-Khatibi F, Avci CB, Salimi L, Bagca BG, Bahador TN, Rezabakhsh A and Khaksar M: Docosahexaenoic acid reversed atherosclerotic changes in human endothelial cells induced by palmitic acid in vitro. Cell Biochem Funct 36: 203-211, 2018.
15. Novinbahador T, Nourazarian A, Asgharzadeh M, Rahbarghazi R, Avci CB, Bagca BG, Ozates NP, Karbasforoush S and Khaki-Khatibi F: Docosahexaenoic acid attenuates the detrimental effect of palmitic acid on human endothelial cells by modulating genes from the atherosclerosis signaling pathway. J Cell Biochem 119: 9752-9763, 2018.
16. Ku CW, Ho TJ, Huang CY, Chu PM, Ou HC and Hsieh PL: Cordycepin Attenuates palmitic acid-induced inflammation and apoptosis of vascular endothelial cells through mediating PI3K/Akt/eNOS signaling pathway. Am J Chin Med 49: 1703-1722, 2021.
17. Tang H, Li K, Zhang S, Lan H, Liang L, Huang C and Li T: Inhibitory effect of paeonol on apoptosis, oxidative stress, and inflammatory response in human umbilical vein endothelial cells induced by high glucose and palmitic acid induced through regulating SIRT1/FOXO3a/NF-κB pathway. J Interferon Cytokine Res 41: 111-124, 2021.
18. Mury P, Chirico EN, Mura M, Millon A, Canet-Soulas E and Pialoux V: Oxidative stress and inflammation, key targets of atherosclerotic plaque progression and vulnerability: Potential impact of physical activity. Sports Med 48: 2725-2741, 2018.
19. Montezano AC and Touyz RM: Reactive oxygen species and endothelial function-role of nitric oxide synthase uncoupling and nox family nicotinamide adenine dinucleotide phosphate oxidases. Basic Clin Pharmacol Toxicol 110: 87-94, 2012.
20. Toualbi LA, Adnane M, Abderrezak K, Ballouti W, Arab M, Toualbi C, Chader H, Tahae R and Seba A: Oxidative stress accelerates the carotid atherosclerosis process in patients with chronic kidney disease. Arch Med Sci Atheroscler Dis 5: e245-e254, 2020.
21. Gryszczynska B, Formanowicz D, Budzyń M, Kossowska MW, Pawliczak E, Formanowicz P, Majewski W, Strzyżewski KW, Kasprzak MP and Iskra M: Advanced oxidation protein products and carbonylated proteins as biomarkers of oxidative stress in selected atherosclerosis-mediated diseases. Biomed Res Int 2017: 4975264, 2017.

22. He F, Li J, Liu Z, Chuang CC, Yang W and Zuo L: Redox mechanism of reactive oxygen species in exercise. Front Physiol 7: 486, 2016.

23. Ji C, Pan Y, Xu S, Yu C, Ji J, Chen M and Hu F: Propolis ameliorates restenosis in hypercholesterolemia rabbits with carotid balloon injury by inhibiting lipid accumulation, oxidative stress, and TLR4/NF-κB pathway. J Food Biochem 45: e13577, 2021.

24. Zhang F, Feng J, Zhang J, Kang X and Qian D: Quercetin modulates AMPK/SIRT1/NF-κB signaling to inhibit inflammatory/oxidative stress responses in diabetic high fat diet-induced atherosclerosis in the rat carotid artery. Exp Ther Med 20: 280, 2020.

25. Li JM and Shah AM: Endothelial cell superoxide generation: Regulation and relevance for cardiovascular pathophysiology. Am J Physiol Regul Integr Comp Physiol 287: R1014-R1030, 2004.

26. Luo S, Wang F, Chen S, Chen A, Wang Z, Gao X, Kong X, Zuo G, Zhou W, Gu Y, *et al*: NRP2 promotes atherosclerosis by upregulating PARP1 expression and enhancing low shear stress-induced endothelial cell apoptosis. FASEB J 36: e22079, 2022.

27. Bennett MR, Sinha S and Owens GK: Vascular smooth muscle cells in atherosclerosis. Circ Res 118: 692-702, 2016.

28. Kirii H, Niwa T, Yamada Y, Wada H, Saito K, Iwakura Y, Asano M, Moriwaki H and Seishima M: Lack of interleukin-1beta decreases the severity of atherosclerosis in ApoE-deficient mice. Arterioscler Thromb Vasc Biol 23: 656-660, 2003.

29. Shimokawa H, Ito A, Fukumoto Y, Kadokami T, Nakaike R, Sakata M, Takayanagi T, Egashira K and Takeshita A: Chronic treatment with interleukin-1 beta induces coronary intimal lesions and vasospastic responses in pigs in vivo. The role of platelet-derived growth factor. J Clin Invest 97: 769-776, 1996.

30. Cagnin S, Biscuola M, Patuzzo C, Trabetti E, Pasquali A, Laveder P, Faggian G, Iafrancesco M, Mazzucco A, Pignatti PF and Lanfranchi G: Reconstruction and functional analysis of altered molecular pathways in human atherosclerotic arteries. BMC Genomics 10: 13, 2009.

31. Chang TT, Yang HY, Chen C and Chen JW: CCL4 inhibition in atherosclerosis: Effects on plaque stability, endothelial cell adhesiveness, and macrophages activation. Int J Mol Sci 21: 6567, 2020.

32. Montecucco F, Lenglet S, Gayet-Ageron A, Bertolotto M, Pelli G, Palombo D, Pane B, Spinella G, Steffens S, Raffaghello L, *et al*: Systemic and intraplaque mediators of inflammation are increased in patients symptomatic for ischemic stroke. Stroke 41: 1394-1404, 2010.

33. Komissarov A, Potashnikova D, Freeman ML, Gontarenko V, Maytesyan D, Lederman MM, Vasilieva E and Margolis L: Driving T cells to human atherosclerotic plaques: CCL3/CCR5 and CX3CL1/CX3CR1 migration axes. Eur J Immunol 51: 1857-1859, 2021.

34. Munjal A and Khandia R: Atherosclerosis: Orchestrating cells and biomolecules involved in its activation and inhibition. Adv Protein Chem Struct Biol 120: 85-122, 2020.

35. Bai HL, Lu ZF, Zhao JJ, Ma X, Li XH, Xu H, Wu SG, Kang CM, Lu JB, Xu YJ, *et al*: Microarray profiling analysis and validation of novel long noncoding RNAs and mRNAs as potential biomarkers and their functions in atherosclerosis. Physiol Genomics 51: 644-656, 2019.

36. Krausgruber T, Blazek K, Smallie T, Alzabin S, Lockstone H, Sahgal N, Hussell T, Feldmann M and Udalova IA: IRF5 promotes inflammatory macrophage polarization and TH1-TH17 responses. Nat Immunol 12: 231-238, 2011.

37. Seneviratne AN, Edsfeldt A, Cole JE, Kassiteridi C, Swart M, Park I, Green P, Khoyratty T, Saliba D, Goddard ME, *et al*: Interferon regulatory factor 5 controls necrotic core formation in atherosclerotic lesions by impairing efferocytosis. Circulation 136: 1140-1154, 2017.

38. Posadas-Sanchez R, Cardoso-Saldaña G, Fragoso JM and Vargas-Alarcón G: Interferon regulatory factor 5 (IRF5) gene haplotypes are associated with premature coronary artery disease. Association of the IRF5 polymorphisms with cardiometabolic parameters. The genetics of atherosclerotic disease (GEA) Mexican study. Biomolecules 11: 443, 2021.

39. Gaubatz JW, Ballantyne CM, Wasserman BA, He M, Chambless LE, Boerwinkle E and Hoogeveen RC: Association of circulating matrix metalloproteinases with carotid artery characteristics: The atherosclerosis risk in communities carotid MRI study. Arterioscler Thromb Vasc Biol 30: 1034-1042, 2010.

40. Polonskaya YV, Kashtanova EV, Murashov IS, Striukova EV, Kurguzov AV, Stakhneva EM, Shramko VS, Maslatsov NA, Chernyavsky AM and Ragino YI: Association of matrix metalloproteinases with coronary artery calcification in patients with CHD. J Pers Med 11: 506, 2021.